Numerical Analysis of Flow Chamber Morphologies for Pilot-Scale Ultrasonication

N. Arunachalam
Process Technology Laboratories, Kaneka Corporation, Takasago, Japan

Introduction: Ultrasonication effectiveness is an important consideration in the scale-up of lab-scale dispersion experiments. Unlike lab-scale experimentation, which can take advantage of localized tools such as probe and bath sonicators, pilot-scale processes may necessitate the use of large flow chambers coupled with powerful ultrasonic wave sources. This situation thus poses the question of whether flow chamber morphology has a salient impact on sonication effectiveness - and if so, what morphologies best optimize the degree of cavitation within flow chambers.

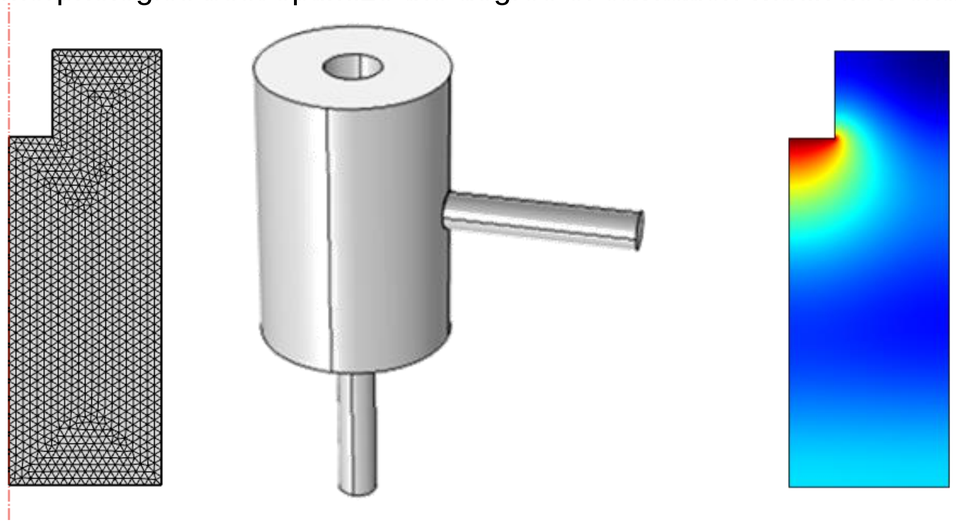

Figure 1. (Left) 2-D axysymmetric model for sonication chamber. (Middle) Illustration of realistic sonication chamber with space for probe at top. (Right) An example acoustic pressure distribution within the sonication vessel.

Background (Sonication Mechanism): The goal of this research is to find sonication chamber geometries that optimize for “acoustic cavitation”, which involves the production of microscopic bubbles in a fluid that produce high-temperature, high-pressure “hotspots” upon explosion. Cavitation bubbles are produced in a liquid if the acoustic pressure is greater than the tensile strength of the liquid; for water, this value is approximately 120 MPa [1].

Computation Methods: A frequency-domain analysis was performed, which uses the following equations and assumptions to obtain an acoustic pressure field:

$$\nabla \cdot -\frac{1}{\rho_c}(\nabla \rho_t - \mathbf{q}_d) - \frac{k_{eq}^2 p_t}{\rho_c} = Q_m$$

$$p_t = p$$

$$k_{eq}^2 = \left(\frac{\omega}{c_c}\right)^2 - \left(\frac{m}{r}\right)^2$$

The geometry walls were defined as sound-hard boundaries except for the upper surface of the probe indentation, which was given a pressure boundary condition. This pressure was calculated from the sonicator power using methods outlined in [2]. A 2D axisymmetric model was used in order to save computation time, and its corresponding mesh is shown in **Figure 1**. The relevant parameters are shown in the group **Table 1** below.

Constant	Value	Units
Density	1000	kg/m3
Speed of Sound	1500	m/s
Temperature	293.15	K

Geom. Param.	Value	Units
R	5	cm
H	10	cm
R_i	1	cm
H_i	2	cm
scale	1	unitless

Variable	Value	Units	Description
P_thresh	120	MPa	Cavitation threshold
f	20	kHz	Sonicator frequency
P	100	W	Sonicator Power

$$I_0 = P/(\pi R_{horn}^2) \qquad \eta \approx 0.85$$

$$p_{boundary} = \sqrt{2 I_0 \eta \rho c}$$

Table 1. (Clockwise from top left) Constants for material (water); parameters related to sonication; intensity equation from [2]; and geometric parameters for vessel.

Sonication Vessel: The geometry of the sonication chamber is shown in **Figure 2** to the right. The fluid is assumed to be water.

Sonication Conditions: The Blake threshold gives a value for the sonicator-induced pressure needed to induce cavitation [3]. A sonication horn radius of 6 mm was assumed. For the default parameters, it was found that the boundary pressure was about 1.5 MPa. Using methods outlined in source [4], the Blake threshold of cavitation for water is determined to be approximately 0.8 MPa.

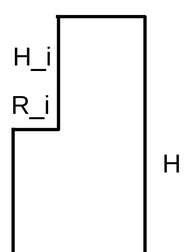

Figure 2. Illustration of parameters involved in 2D axisymmetric model.

Results: Cavitation regions were defined as regions in which acoustic pressure exceeds the Blake threshold of cavitation. Some example cavitation regions are shown in **Figure 3** below for a geometry scan of vessel diameter:

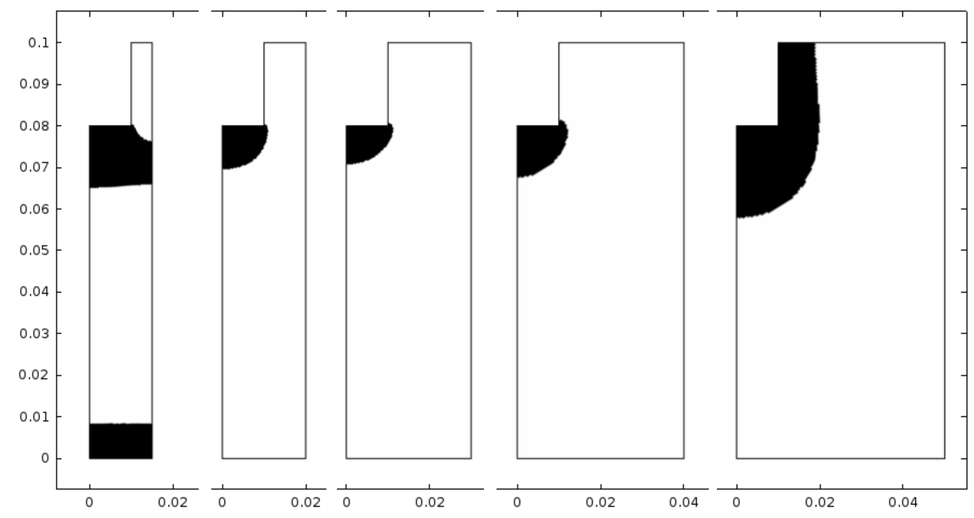

Figure 3. Cavitation regions for a parameter scan of R (from left to right: R = 1.5 cm, 2 cm, 3 cm, 4 cm, 5 cm). Note that some geometries optimize the area of the cavitation region more than others; for example, a greater cavitation volume is observed for R = 5 cm than for R = 2, 3, and 4 cm.

If we assume a constant flow rate of f and a total volume of V, then we expect a residence time of T = V/f. The probability of a particle being within the cavitation region is proportional to the volume of the cavitation region divided by V. Thus, the extent of sonication experienced by each particle leaving the sonication chamber (and thus the sonication effectiveness) is proportional to the volume of the cavitation region.

There are three main variables that can be manipulated: the depth of the probe, the height of the vessel, and the diameter of the vessel. The radius of the probe is assumed constant. To observe the effect of manipulating these parameters, parameter scans were made keeping all

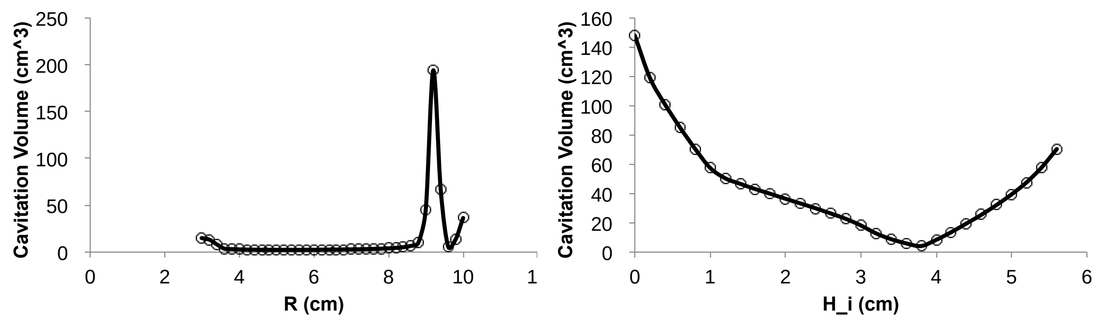

Figure 4. Variation in cavitation volume during parameter sweep. Notice that a peak in cavitation volume occurs at R = 9.2 cm, all other geometric parameters held constant. Optimal sonication probe height appears to be surface-level. The asymmetry in the H_i curve can be attributed to the volume taken up by the probe itself, which detracts from sonication volume.

Conclusions: The methods used in this research are applicable to a wide variety of fluids [5] due to the ability of COMSOL to adapt to analyze materials with different densities and sound speeds. The main result of this research is to demonstrate that sonication effectiveness is highly contingent on geometry; for example, as seen in **Figure 4**, large changes can be observed in sonication quality based on changes in geometric parameters. Size-depended effects,, like with R = 9.2 cm, in the figure, can make sonication orders of magnitude more effective.

For the specific combination of parameters used in this study, which are derived from commercially available materials, knowing how variations in geometry can effect sonication effectiveness can yield large dividends in the scale-up of industrial processes. From a design perspective, these results will be useful for creating more effective sonication setups

References:

1.E. Herbert, et al., “Cavitation Pressure in Water”, *Physical Review E*, 74, 1-32 (2006).
2.S. Dahnke, F. J. Keil, “Modeling of Three-Dimensional Linear Pressure Fields in Sonochemical Reactors with Homogeneous and Inhomogeneous Density Distributions of Cavitation Bubbles”, *Ind. Eng. Chem. Res.*, 37, 848-864 (1998).
3.H. Feng, G. V. Barbosa-Canovas, “Ultrasound Technologies for Food and Bioprocessing”, *Springer Print*, 1-16 (2011).
4.A. Atchley, “The Blake threshold of a cavitation nucleus having a radius-dependent surface tension”, *J. Acoust. Soc. Am.*, 85, 152-157 (1989).
5.T.Y. Wu, et al., “Advances in Ultrasound Technology for Environmental Remediation”, *Springer Print*, 1-12 (2013).

Excerpt from the Proceedings of the 2017 COMSOL Conference in Singapore